Comparisons of echo-integration performance from two multiplexed echosounders

Gavin J. Macaulay [1,*], Ben Scoulding[2,3], Egil Ona[1], and Sascha M. M. Fässler[3,4]

[1]*Institute of Marine Research, Bergen, Norway*
[2]*Oceans and Atmosphere Flagship, Commonwealth Scientific and Industrial Research Organisation, GPO Box 1538, Hobart, TAS 7001, Australia*
[3]*Wageningen Marine Research, Haringkade 1, 1976 CP IJmuiden, The Netherlands*
[4]*Cantonal Office for Environment and Energy Basel-Stadt, Hochbergerstrasse 158, 4019 Basel, Switzerland*

Corresponding author: tel: +47 47 97 35 70; e-mail: gavin.macaulay@hi.no.

A time-series of acoustically derived aquatic biomass estimates relies on the acoustic equipment maintaining the same performance throughout the time-series. This is normally achieved through a regular calibration process. When the acoustic equipment changes it is necessary to verify that the new equipment produces a similar result to the old equipment, otherwise an unknown bias can be introduced into the time-series. The commonly used Simrad EK60 echosounder has been superseded by the Simrad EK80 echosounder and the performance of these two scientific echosounder systems was compared using interleaved pinging through the same transducer. This was repeated for multiple transducer frequencies (18, 38, 70, 120, and 200 kHz) and from two vessels (Norway's G.O. Sars in the North Sea and The Netherlands' Tridens in the Northeast Atlantic Ocean). The broadband facility of the EK80 was not used. Regressions of the grid-integrated backscatter from the two systems were highly linear. The difference in area backscattering coefficients in typical survey conditions was less than 0.6 dB (12%) at the main survey frequency of 38 kHz. In most conventional fish acoustic surveys, the observed differences are less than other sources of survey bias and uncertainty.

Keywords: acoustic survey, echo-integration, echosounder, EK60, EK80, intercomparison

Introduction

The management of fisheries typically requires unbiased estimates of population sizes over many years. For some fish stocks, these estimates can be obtained by acoustic surveys, where calibrated sonar systems are used to measure the reflectivity of fish aggregations (Simmonds and MacLennan, 2005). With knowledge of individual fish reflectivity, estimates of fish numbers and hence population size can be derived. The most common tool used for acoustic surveys of fish is the mono-static echosounder mounted on a moving platform, often a ship, which is used to conduct a systematic survey. The echosounder measurements are used to estimate the mean volume-normalized backscatter per unit area of water surface, termed the area backscattering coefficient, s_a ($m^2\,m^{-2}$) (MacLennan et al., 2002).

Fisheries assessment models take, as an input, a time-series of biomass estimates obtained from surveys (Hilborn and Walters, 2003). These estimates need not be absolute estimates, but must be comparable across surveys. This requires that any bias or method assumptions remain constant or known from survey to survey. An important comparability requirement for acoustic surveys is that the echosounder is calibrated, and that multiple echosounders and platforms would provide the same backscatter results from the same organisms. This is easily achieved when a single platform and echosounder is used consistently over many surveys, but when the echosounder is changed, great care is necessary to ensure that comparable results are obtained (Jech et al., 2005).

A very commonly used echosounder transceiver for fisheries surveys is the Simrad EK60, commercially available since the year

2001 (Andersen, 2001). The manufacturer has recently replaced it with a new model, the EK80. As new survey platforms are built and as maintenance of the EK60 becomes difficult due to unavailability of spare parts and the eventual ending of manufacturer support, fisheries acoustics surveys will likely migrate to the use of EK80 echosounders. The EK80 has a different hardware and software design to the EK60 and validation that the EK80 gives near-identical results to the EK60 is an essential prerequisite to the use of EK80s for quantitative acoustic surveys, especially when the results contribute to an existing survey time-series. If they do not give near-identical results, an understanding of the magnitude and characteristics of any differences will enable an assessment of potential effects on survey estimates and suggest ways to compensate for any differences.

The production of fish biomass estimates involves a chain of equipment and software-based processing. The entire chain should be verified when one component changes, as a change in one part often requires changes in other parts (e.g. a new echosounder can have a different data file format and provide the backscatter data in a different form). For acoustic surveys, this includes the software programs used to calibrate and operate the echosounder, as well as those that process the echosounder data to produce biomass estimates.

This paper tests the hypothesis that backscatter measurements derived from the EK60 and EK80 echosounders are near-identical. This was achieved by collecting interleaved datasets from two multifrequency echosounders operating through the same transducers and processed using existing software programs over a wide range of organism types and densities.

Methods

Contemporary data were collected from Simrad EK60 and Simrad EK80 echosounders by connecting an EK60 transceiver to a hull-mounted transducer for a single ping, then connecting an EK80 transceiver to the same transducer for the subsequent ping. This cycle was then repeated. This is termed multiplexing, where the one transducer is switched between two transceivers. The work presented here uses the narrowband mode of the EK80 as this is the same mode of operation as the EK60. Narrowband mode uses short transmit pulses that are nominally at a single frequency, but due to finite pulse durations have a bandwidth of several kHz (the EK80 can also generate and process broadband pulses that, when combined with a transducer, can have bandwidths about between 10 and 200 kHz).

Multiplexed backscatter data were collected by two vessels, RV G.O. Sars (Norway) and RV Tridens (The Netherlands) through a range of transducers operating at 18, 38, 70, 120, and 200 kHz, namely Simrad models ES18, ES38B, ES70-7C, ES120-7C, and ES200-7C. The system on G.O. Sars was only able to multiplex one transducer at a time because manual reconfiguration was required to move the multiplexing equipment between transducers and transceivers. All EK60 channels transmitted simultaneously, then the connected EK80 channel, then the EK60 channels, etc. The multiplexed EK80 channel was changed after sufficient pings had been collected. The system on Tridens could multiplex all transducers simultaneously, but only one EK60 and EK80 transceiver pair was set to actively transmit at a time to prevent crosstalk between channels.

The echosounders were calibrated through the multiplexing system, using the standard sphere method (Demer et al., 2015), with the same operating parameters for the EK60 and EK80 (Table 1a and 1b). The 200 kHz channel on Tridens was not calibrated through the multiplexing system and was excluded from the analysis. The echosounders on G.O. Sars were calibrated in Byfjorden,

outside of Bergen harbour, Norway on 5 November 2015, while those on Tridens were calibrated in Little Loch Broom on the northwest coast of Scotland on 2 April 2016. The calibration analysis was carried out using the echosounder-specific software provided by the manufacturer and then converted into calibration files of the form required by the analysis programs. Versions 2.4.3 and 1.12.1 of the EK60 and EK80 software, respectively, were used on G.O. Sars, while versions 2.4.3 and 1.8.3.0, respectively, were used by Tridens. To ensure that the EK60 and EK80 used the same calibration sphere target strength, the value that the EK80 calculates was manually input to the EK60 calibration process. Similarly, the same sound speed and acoustic absorption values were used for the EK60 and EK80 datasets. The standard sphere calibration method as implemented by the EK60 and EK80 does not provide estimates of equivalent beam angle and manufacturer-provided values were used. The assumption was made that the EK60 and EK80, when operating through the same transducer, produced an acoustic field with the same equivalent beam angle.

The multiplexing hardware differed between vessels, but both used computer-controlled mechanical relays to switch the transducer cable between the echosounder transceivers. The multiplexer computer triggered the transmit and receive operations of the appropriate transceiver via the trigger input serial port on the computers running the EK60 and EK80 programs. The switching between transceivers took about 6 ms and the per-echosounder ping rate varied between 0.3 and 1 Hz.

Acoustic data were collected opportunistically from G.O. Sars during operations in the North Sea in November 2015. Line transect data were collected for each transducer over a range of acoustic marks (Figure 1), including dense Atlantic mackerel (Scomber scombrus) aggregations and layers, low amplitude background layers, and resolved echoes from individual fishes. Vessel speed varied between 0 and 6.3 ms^{-1}. The maximum bottom depth was 110 m. Additional data were collected in November 2017 from G.O. Sars without simultaneous EK60 transmission on all channels. These data were at 38 and 70 kHz over a seafloor depth of about 250 m in the fjord area to the northeast of Tromsø, Norway.

Acoustic data were collected by Tridens during the Dutch component of the International Council for the Exploration of the Sea (ICES) coordinated International Blue Whiting Spawning stock Survey (IBWSS) in March 2016. Data were collected while the ship was moving between the survey transects. Vessel speed varied between 4.6 and 5.7 ms^{-1}. Tridens collected data from a variety of different acoustic marks and scattering layers (Figure 2), loosely divided into: (1) blue whiting (Micromesistius poutassou) layers of various densities at depths between 300 and 600 m, (2) blue whiting schools with medium to high densities around 300–500 m, (3) Mueller's pearlside (Maurolicus muelleri) layers around 100–200 m, (4) layers and aggregations of plankton throughout the water column, and (5) Atlantic mackerel schools from the surface down to around 300 m. Data were collected down to a depth of 700 m.

The data quality from both vessels was very good and the only pre-processing was the removal of a small number of noise-dominated pings in the Tridens dataset. Background noise estimates were estimated from sections of data when the echosounder channels were set to passive mode or from ranges below the bottom echo using the De Robertis and Higginbottom (2007) method.

Data from G.O. Sars were integrated with the LSSS computer program (version 2.3.0, Korneliussen et al., 2016) and data from Tridens were integrated using the Echoview computer program (version 8.0.86, Echoview Software Pty Ltd, Hobart, Tasmania). All

Table 1a. Echosounder operating parameters, calibration summary, and background noise estimates for the 18, 38, and 70 kHz channels on RV G.O. Sars and RV Tridens.

Parameter	Units	Values											
Frequency	kHz	18				38				70			
Ship		G.O. Sars		Tridens		G.O. Sars		Tridens		G.O. Sars		Tridens	
Echosounder		EK60	EK80	EK60	EK80	EK60	EK80	EK60	EK80	EK60	EK80	EK60	EK80
Pulse duration	ms	1.024	1.024	1.024	1.024	1.024	1.024	1.024	1.024	1.024	1.024	1.024	1.024
Transmit power	W	2000	2000	2000	2000	2000	2000	2000	2000	800	800	750	750
Equivalent beam angle	dB re 1 sr	−17.3	−17.3	−17.0	−17.0	−20.8	−20.8	−20.6	−20.6	−20.6	−20.6	−21.0	−21.0
Calibration gain	dB re 1	21.77	22.08	22.92	23.87	25.28	25.64	26.55	27.54	26.84	28.18	26.99	28.25
S_a correction	dB re 1	−0.59	0.00	−0.76	−0.02	−0.61	−0.05	−0.64	−0.01	−0.41	−0.01	−0.38	0.00
Beam model fit root-mean-square error	dB	0.3	0.08	0.15	0.07	0.1	0.04	0.10	0.04	0.1	0.13	0.10	0.04
Beam angle, athwartship	°	10.6	11.5	10.8	11.5	7.2	7.5	6.5	6.5	6.6	6.6	6.5	6.6
Beam angle, alongship	°	11.5	12.7	10.7	11.5	7.2	7.5	6.5	6.5	6.7	6.7	6.5	6.7
Beam offset, athwartship	°	−0.3	−0.2	−0.1	0.1	−0.1	0.0	−0.0	0.0	−0.1	−0.0	−0.0	−0.0
Beam offset, alongship	°	0.0	−0.5	0.0	0.1	0.2	−0.1	−0.1	0.1	0.0	0.0	−0.1	0.0
Sphere material		Cu	Cu	Cu	Cu	Cu	Cu	WC	WC	WC	WC	WC	WC
Sphere diameter	mm	64	64	63	63	60	60	38.1	38.1	38.1	38.1	38.1	38.1
Sphere range	m	30	30	15	17	26	26	10	10	21	21	10	10
Background noise ($Power_{cal}$)	dB	−153	−117	−149	−148	−166	−132	−146	−145	−167	−148	−163	−150

Table 1b. Echosounder operating parameters, calibration summary, and background noise estimates for the 120 and 200 kHz channels on RV G.O. Sars and RV Tridens.

Parameter	Units	Values					
Frequency	kHz	120				200	
Ship		G.O. Sars		Tridens		G.O. Sars	
Echosounder		EK60	EK80	EK60	EK80	EK60	EK80
Pulse duration	ms	1.024	1.024	1.024	1.024	1.024	1.024
Transmit power	W	250	250	250	250	150	150
Equivalent beam angle	dB re 1 sr	−21.0	−21.0	−21.0	−21.0	−20.5	−20.5
Calibration gain	dB re 1	26.62	26.79	27.06	27.50	26.56	27.82
S_a correction	dB re 1	−0.34	−0.02	−0.31	−0.01	−0.32	0.01
Beam model fit root-mean-square error	dB	0.1	0.06	0.1	0.0	0.2	0.2
Beam angle, athwartship	°	6.6	6.6	6.5	6.5	6.7	6.5
Beam angle, alongship	°	6.5	6.5	6.5	6.6	6.3	6.2
Beam offset, athwartship	°	0.1	0.0	0.0	0.1	0.0	0.1
Beam offset, alongship	°	0.0	0.1	0.1	0.1	−0.2	−0.0
Sphere material		WC	WC	WC	WC	WC	WC
Sphere diameter	mm	38.1	38.1	38.1	38.1	38.1	38.1
Sphere range	m	21	21	10	10	28	28
Background noise ($Power_{cal}$)	dB	−155	−151	−141	−144	−153	−150

of the G.O. Sars data were also processed with Echoview to provide a comparison between the outputs of these two programs. The programs were used to identify common regions, in time and depth, between the EK60 and EK80 data. Volume backscattering coefficients (MacLennan *et al.*, 2002), s_v (m^2 m^{-3}), were integrated into area backscattering coefficients (s_a, m^2 m^{-2}) at a vertical and horizontal grid resolution of 5 m and 102 s, respectively (the only way to specify the same grid starting ping in LSSS and Echoview was to use time as the grid unit and as Echoview requires grid size as minutes to 1 decimal place and LSSS as integer seconds, 102 s was the closest common value to the desired 100 s horizontal grid size). Both programs applied vessel heave before integrating into the grid. When present, the bottom echo was included in the integration regions to give high amplitude echoes for the comparison. All data less than 20 m below the surface were excluded to avoid transducer ringdown [the echosounder transducers were 8.5 m (G.O. Sars) and 8.6 m (Tridens) below the surface via the use of lowerable keels]. Where appropriate, the logarithmic version of the area backscatter coefficient, the area backscattering strength (S_a, dB re 1 m^2 m^{-2}) has been used.

Ideally, a comparison of echosounder performance should be carried out on a range of homogenous backscattering layers with slowly changing densities that minimize the effect of spatial variability on the comparison, as is recommended for the similar process of inter-calibration of echosounders on separate vessels (Simmonds and MacLennan, 2005). However, such scattering conditions are difficult to find, and real-world comparisons combine the effect of equipment performance (the purpose of this paper) with spatial variation in the backscatter and platform motion
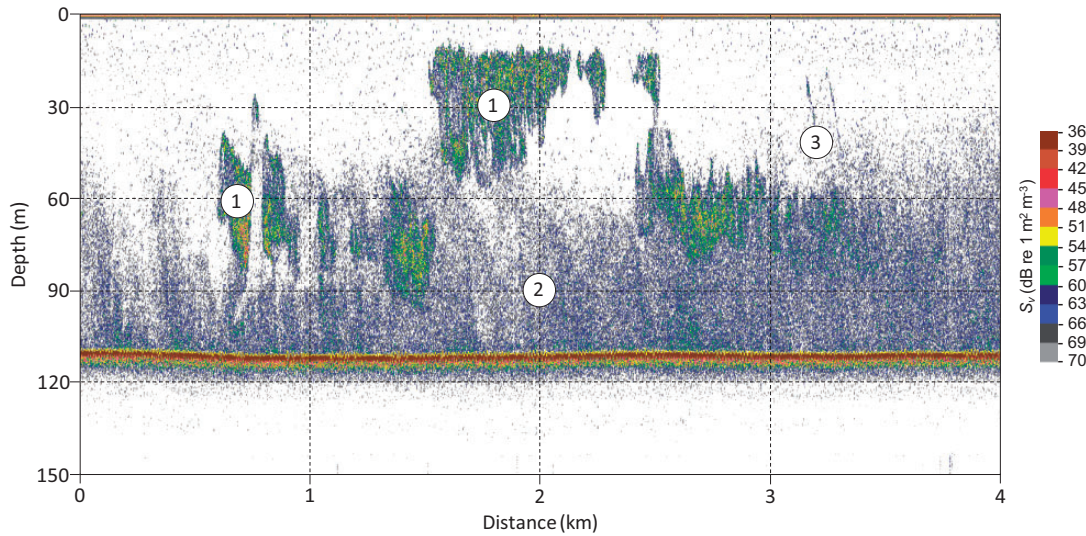
Figure 1. Echogram of volume backscattering strength (S_v, dB re 1 m^2 m^{-3}) at 38 kHz showing the key mark types observed by RV G.O. Sars; (1) dense Atlantic mackerel (*S. scombrus*) aggregations and layers from the surface to 100 m, (2) low amplitude background layers from 50 m to the seabed, and (3) resolved echoes from individual fishes throughout the water column.
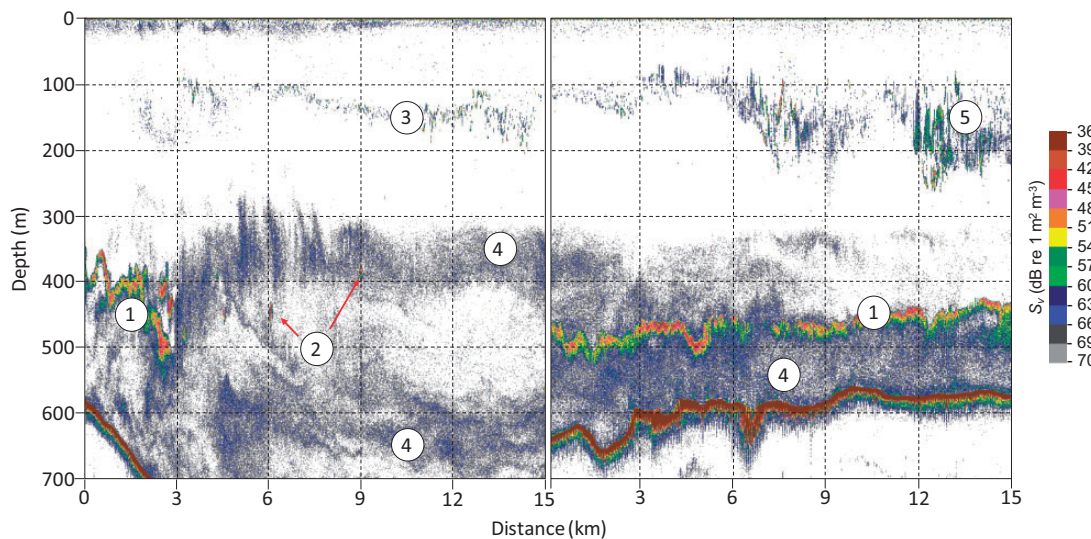

Figure 2. Echogram of volume backscattering strength (S_v, dB re 1 m^2 m^{-3}) at 38 kHz showing the five key mark types observed by RV Tridens; (1) blue whiting (*M. poutassou*) layers of various densities at depths between 300 and 600 m, (2) blue whiting schools with medium to high densities around 300–500 m, (3) Muellers pearlside (*M. muelleri*) layers around 100–200 m, (4) layers and aggregations of plankton throughout the water column, and (5) Atlantic mackerel (*S. scombrus*) schools from surface down to around 300 m.

between successive echosounder pings. For this study, the effect of platform motion and non-homogenous layers was quantified by splitting a subset of the EK60 datasets into two datasets, thereby removing the effect of equipment performance. A custom-written program was used to move every second ping in the EK60 datafiles into separate files, thereby simulating a multiplexed configuration with two identical echosounders. Echo-integration was then carried out in the same manner as for the EK60/EK80 datasets. Due to the splitting of the EK60 datasets, the effective ping rate of the split dataset was half that of the EK60/EK80 datasets.

The differences between the echo-integrals from the EK60 and EK80 echosounders were compared with several metrics, applied separately to each echosounder frequency:

Metric 1: The linearity between systems was tested by fitting a robust linear regression [using an iteratively reweighted least squares algorithm (Holland and Welsch, 1977)] to the pairs of area backscattering coefficients. Variability of the data points about the regression was assessed using the root-mean-square error (RMSE).

Metric 2: The differences between the fitted robust linear regression and the ideal one-to-one regression (at EK60 area backscattering strength values of −70 and −30 dB re 1 m^2 m^{-2}) were calculated. This gives an estimate of the differences at two representative fisheries survey backscatter values.

Metric 3: The stochastic model of Kieser *et al.* (1987) was applied to test the null hypothesis of equal echo-integrals.

The model yields an estimate, R, with 95% confidence intervals, which is the ratio of population estimates obtained from the two echosounders, under some assumptions about the statistical properties of the input. It will be approximately 1.0 if the measurements are the same.

Table 2. Vessel distance travelled per frequency when collecting the EK60/EK80 datasets.

Frequency (kHz)	RV G.O. Sars Distance (km)	RV Tridens Distance (km)
18	51	116
38	68	114
70	51	56
120	152	14
200	362	–

Results

The echosounder calibrations gave results that were consistent with previous calibrations. The variability of the calibration sphere echo strength about the ideal beam pattern was small (Table 1a and 1b, "Beam model fit root-mean-square error" row), indicating good quality calibrations. A total of 684 km of data were collected by G.O. Sars and 300 km from Tridens (Table 2) for the EK60 to EK80 comparison. The split EK60 comparison of G.O. Sars data was obtained from 47 km of transects and the split Tridens comparison from 54 km of transects.

The grid integrals were closely clustered around the 1:1 line (Figure 3) and had good qualitative agreement in the shape, size, and location of scattering regions (Figure 4), including the bottom echo when visible. The split EK60 and EK60 to EK80 regression slopes were all close to 1.0 (Metric 1; Table 3). The RMSE of the regressions varied between 0.3 and 1.2 dB re 1 m^2 m^{-2} for G.O. Sars and between 0.7 and 1.9 dB re 1 m^2 m^{-2} for Tridens. The area
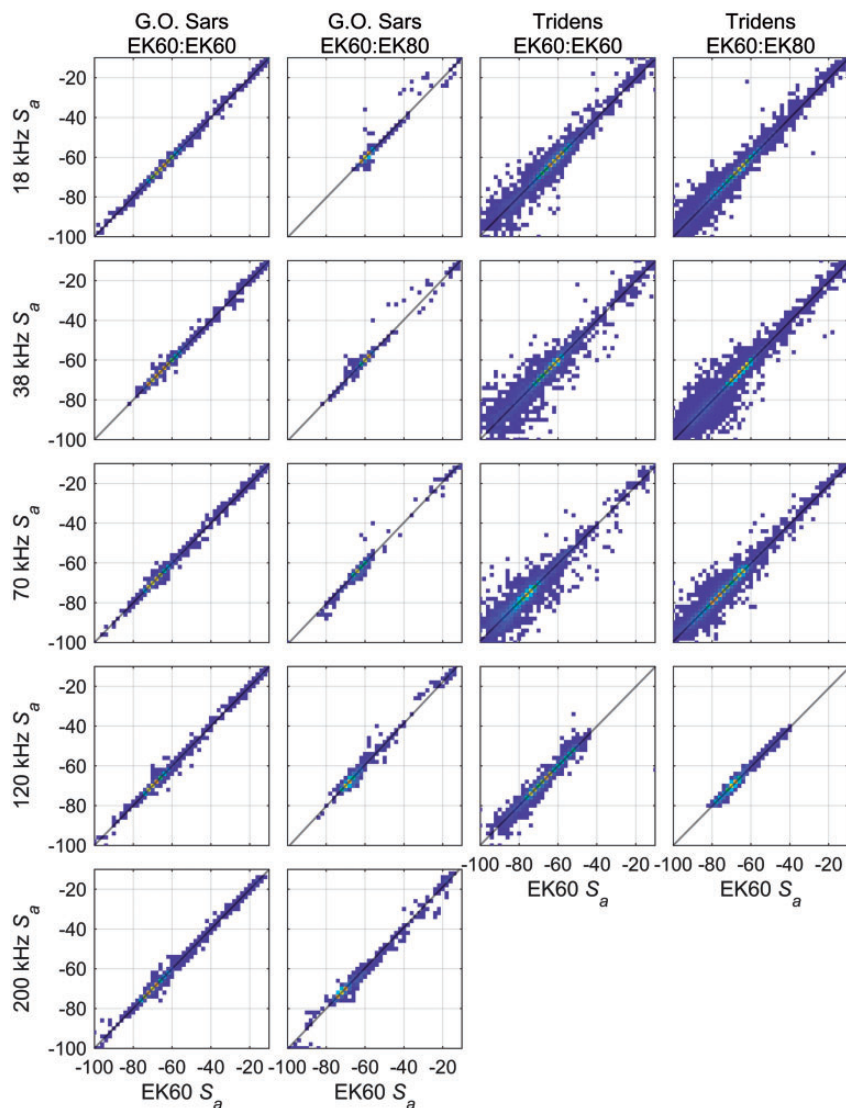

Figure 3. Two-dimensional histogram of area backscattering strength (S_a, dB re 1 m^2 m^{-2}) cell pairs from the EK60 to EK60 and EK60 to EK80 comparisons for RV G.O. Sars and RV Tridens. Colour indicates the number of cell pairs in the 2 dB by 2 dB histogram grid, where blue is the lowest and yellow the highest (dark to light in greyscale). The solid line is the fitted regression to the data.

backscattering strength (S_a, dB re 1 m^2 m^{-2}) differed by more than 40 dB re 1 m^2 m^{-2} in a few grid cells, which contained abrupt changes in backscatter with time or depth (Figures 3 and 4), such as from the seafloor. Most S_a values were between -70 and -60 dB re 1 m^2 m^{-2}, reflecting the background area backscatter strength in the data collection areas, while the bottom echo produced a group of S_a values above -20 dB re 1 m^2 m^{-2} (Figure 3).

There were systematic differences in the cell-to-cell S_a comparison, such as the string of points that extended below the 1:1 line in the G.O. Sars 200 kHz dataset (Figure 3). Both datasets had range-related trends in the S_a difference, most obviously for the G.O. Sars EK60 to EK80 datasets at 120 and 200 kHz and for the Tridens data at 70 and 120 kHz at larger ranges (Figure 5). Notable differences also occurred closer than 40 m to the transducer, and near the bottom echo (105–140 m) for the G.O. Sars
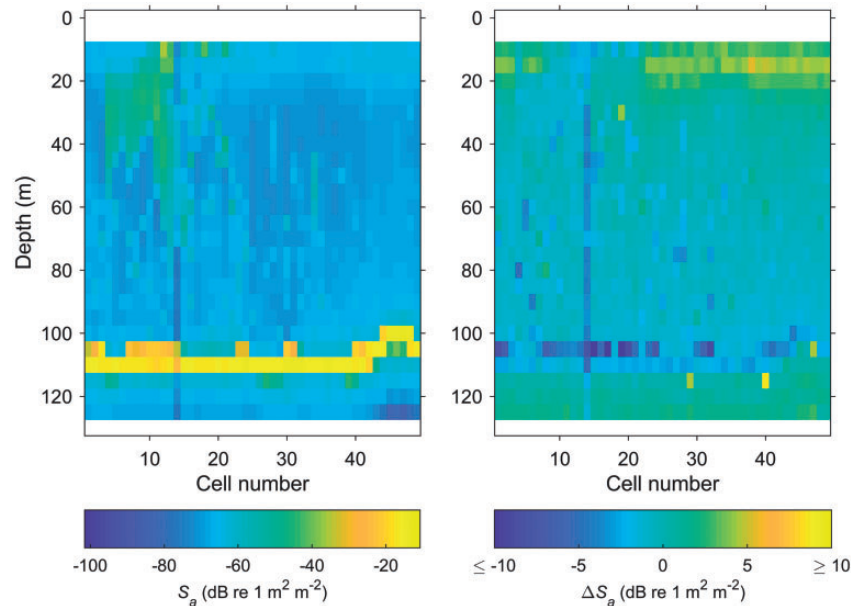

Figure 4. Gridded area backscattering strength (S_a, dB re 1 m^2 m^{-2}) data from the RV G.O. Sars 120 kHz dataset (EK60, left panel) and per-cell difference (EK60–EK80) to the EK80 dataset (right panel). The bottom echo generates the strong backscatter at 110 m and a dense aggregation of fish generates the increased backscatter between 10 and 60 m over cell numbers 3–15.

Table 3. Comparisons between the echo-integrals of the split EK60/EK60 and EK60/EK80 datasets for RV G.O. Sars and RV Tridens.

| Frequency (kHz)	Comparison type	Vessel	Processing software	Regression slope	Root-mean-square error (dB)	Kieser R ratio	Diff. at $S_a = -70$ (dB)	Diff. at $S_a = -30$ (dB)	No. cells
18	EK60/EK60	G.O. Sars	LSSS	1.00	0.3	1.00	0.0	0.0	3 323
		Tridens	Echoview	1.00	1.4	1.00	0.0	0.2	2 622
	EK60/EK80	G.O. Sars	LSSS	1.01	0.5	1.05	0.1	0.3	332
			Echoview	1.01	0.5	1.04	0.1	0.4	257
		Tridens	Echoview	1.00	0.8	1.12	0.2	0.4	2 163
38	EK60/EK60	G.O. Sars	LSSS	1.00	0.4	1.00	0.0	0.0	3 340
		Tridens	Echoview	0.99	1.9	0.99	0.0	0.4	2 991
	EK60/EK80	G.O. Sars	LSSS	1.02	0.4	0.99	-0.5	0.2	357
			Echoview	1.01	0.4	0.97	-0.4	0.1	293
		Tridens	Echoview	1.00	0.9	1.15	0.6	0.6	5 163
70	EK60/EK60	G.O. Sars	LSSS	1.00	0.4	1.00	0.0	0.0	3 329
		Tridens	Echoview	0.95	1.7	0.95	0.4	2.6	1360
	EK60/EK80	G.O. Sars	LSSS	1.02	0.6	0.96	-0.6	0.3	350
			Echoview	1.02	0.6	0.95	-0.7	0.3	291
		Tridens	Echoview	0.97	1.3	0.97	0.2	1.6	4 801
120	EK60/EK60	G.O. Sars	LSSS	1.00	0.4	1.00	0.0	0.1	3 300
		Tridens	Echoview	0.98	1.0	1.01	0.1	1.0	1 178
	EK60/EK80	G.O. Sars	LSSS	1.04	1.2	0.82	-1.8	-0.1	515
			Echoview	1.04	1.0	0.82	-2.0	-0.3	476
		Tridens	Echoview	1.00	0.7	1.26	0.9	0.9	598
200	EK60/EK60	G.O. Sars	LSSS	1.00	0.4	1.00	0.0	0.1	3 310
	EK60/EK80	G.O. Sars	LSSS	1.02	1.2	0.83	-1.0	-0.2	965
			Echoview	1.02	1.1	0.83	-1.1	-0.4	801
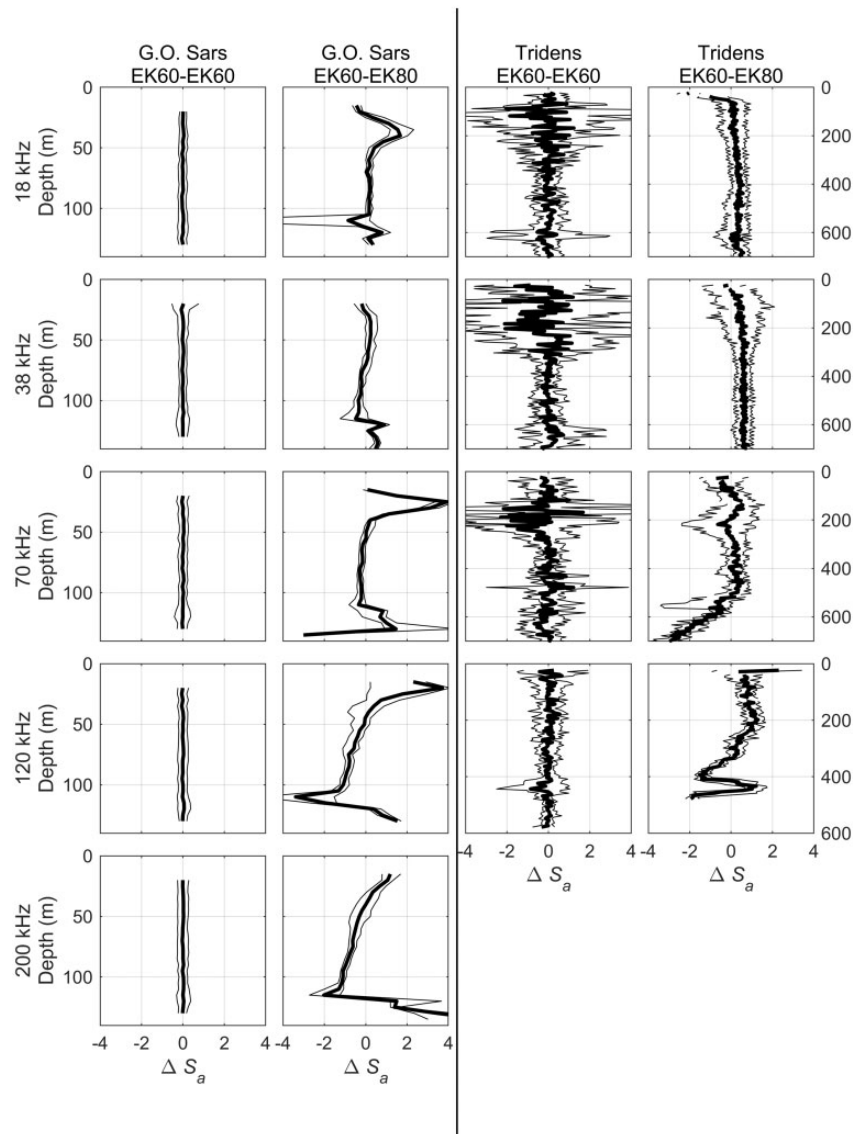
Figure 5. Variation with depth (solid thick line) of the median of the difference (EK60–EK80) in cell S_a (dB re 1 m^2 m^{-2}) values for the EK60 to EK60 and EK60 to EK80 datasets for RV G.O. Sars and RV Tridens. Also shown are the 25% and 75% percentiles (thin black lines) of the differences.

dataset. These differences were not present in the Tridens dataset. The Tridens datasets had a much larger variation than for G.O. Sars (Figures 3 and 5).

The difference between the fitted linear regression and the 1:1 line (Metric 2) at $S_a = -70$ dB varied between -2.0 and 0.9 dB and at $S_a = -30$ dB between -0.4 and 2.6 dB.

The Kieser *et al.*, R ratio (Metric 3) for the EK60 to EK80 datasets ranged from 0.82 to 1.26 over all comparisons, while the R ratios for the split EK60 datasets were always within 0.05 of unity (Table 3). The 95% confidence interval on R was always smaller than ± 0.05. Consistent differences in performance between the EK60 and EK80 echosounders occurred at ranges less than 50 m and at and below the bottom echo (Figure 4). Backscatter from these regions was hence excluded from the EK60 to EK80 R ratio.

Differences in how Echoview and LSSS defined the integration grid made direct cell-to-cell comparisons infeasible. However, the

regressions derived from the EK60 to EK80 S_a values agreed closely between Echoview and LSSS (Table 3). The EK80 background noise levels were higher than the EK60 on both vessels, except for the 120 kHz on Tridens (Tables 1a and 1b). In particular, the G.O. Sars EK80 levels were significantly higher than the EK60 at some frequencies.

Discussion
The close agreement of the split G.O. Sars EK60 dataset and the more variable results seen in the Tridens data (Figure 3) over restricted depth ranges (Figure 5) highlights the dependence of the *in situ* multiplexing method on adequate spatial homogeneity in the backscatter (for Tridens the higher variability was caused by layers of small dense aggregations that varied significantly from ping to ping, as illustrated by mark types 3 and 5 in Figure 2). The split dataset was taken from similar time periods and locations as the EK60 to EK80 datasets and hence can be used as a baseline for the EK60 to

EK80 comparison. Differences beyond those observed in the split comparison can then be attributed mostly to differences in performance of the EK60 and EK80 echosounders and data processing.

A direct comparison of the total backscattered energy received by the two echosounders may appear to be a useful way to compare the two echosounders. However, due to the very wide range of backscatter amplitudes (exceeding a factor of 100 000), the summation is dominated by grid cell integrals with high backscatter and a total integral comparison is dominated by backscatter from strong targets. The difference at specific EK60 S_a values provides instead a measure of the expected range in differences between the EK60 and EK80 and is not directly dependent on the distribution of backscatter values observed during our experiments, as the summation would be.

The overall comparison between the EK60 and EK80 shows close agreement, but there are some situations where the agreement is poor. An understanding and awareness of these situations and their magnitude is important when using an EK80 to replace an EK60 for quantitative time-series analyses. Note that, in general, the multiplexing comparison method does not indicate which echosounder is the most correct.

The differences that occur at ranges of less than 40 m to the transducer (Figure 5) in the G.O. Sars data starts after the transducer ringdown and decreases gradually as the range increases and was not visible in the data from Tridens. There was good agreement in the full-resolution (i.e. unintegrated) sample data, but when the difference was apparent the EK60 values were always higher than the EK80 values. A plausible explanation is cross-channel harmonic and subharmonic interference due to the configuration of the EK60 on G.O. Sars—the multiplexing setup on G.O. Sars produced an EK60 transmission on all transducers simultaneously (18, 38, 70, 120, and 200 kHz), while the EK80 transmission only occurred on one transducer. The echosounder configuration on Tridens did not transmit on all EK60 transducers simultaneously and hence there was no possibility for cross-channel interference.

There was also a several dB difference associated with the bottom echo (Figure 5). This was most obvious in the G.O. Sars dataset where the bottom depth was consistently between 100 and 110 m, compared to the Tridens dataset where the bottom depth was often greater than 700 m and not included in the comparisons. Both the bottom echo and the associated reverberation differed between the EK60 and EK80 (Figure 4). Some of these differences would be due to small offsets in bottom depth that shift high amplitude backscatter data between integration grid cells. However, the full-resolution sample data showed that the peak of the bottom echo was up to 1 dB lower on the EK60. The post-peak reverberation was generally higher on the EK60 except for the 18 kHz channel where it was similar and could be caused by the same cross-channel interference as postulated for the G.O. Sars near-transducer differences. The small dataset collected from G.O. Sars without simultaneous multitransducer EK60 transmission did not show the short range and near-bottom differences between the EK60 and EK80 (Figure 6), indicating that the differences observed in the main dataset were due to cross-talk between channels.

The EK80 system used for our measurements generates in-water pulses that can differ from the EK60. This includes the time taken to reach full transmit power, the rate of transmit power decrease during the pulse duration, and the rate of decrease in transmit energy at the end of the pulse (Demer *et al.*, 2017). The calibration process is energy-based in both echosounders and
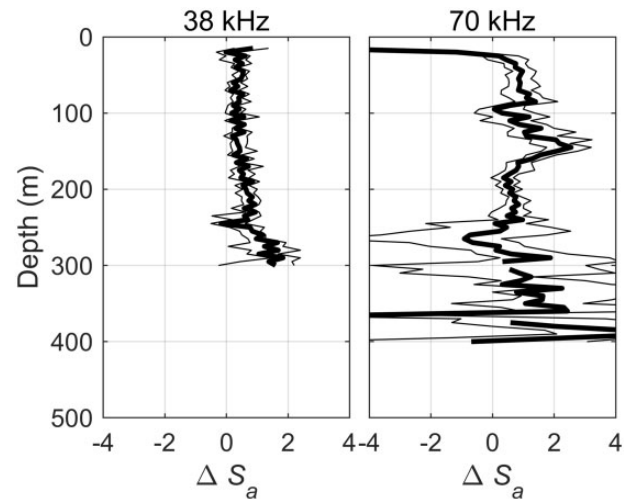

Figure 6. Variation with depth (solid thick line) of the median of the difference (EK60–EK80) in cell S_a (dB re 1 m^2 m^{-2}) values for the November 2017 G.O. Sars EK60 to EK80 datasets where channel crosstalk was prevented by only operating one EK60 channel at a time. Also shown are the 25% and 75% percentiles (thin black lines) of the differences.

such differences should ideally be removed by the calibration, but some small differences can remain.

The multiplexing systems prevented adherence to the recommended electrical shielding and grounding arrangement of the echosounder systems and this led to increased levels of background noise in the EK60 and EK80 datasets, but more so for the EK80. The current-day EK80 installation on G.O. Sars (without multiplexing) has considerably lower noise levels than measured during the multiplexing measurements.

There was a pronounced depth-dependent variation in the G.O. Sars 120 and 200 kHz and Tridens 70 and 120 kHz datasets (Figure 5), where the amount of energy in the EK80 data increased in comparison to the EK60 data with increasing range. However, viewing the differences as a function of calibrated received power at the transducer [$Power_{cal}$, obtained by subtracting the sonar equation spherical spreading and absorption corrections from S_a (De Robertis and Higginbottom, 2007)], shows that the difference occurs at low received power levels for Tridens (Figure 7) and can be attributed to differing low level noise characteristics of the EK60 and EK80 echosounders. The 120 and 200 kHz G.O. Sars datasets have a steady increase in the relative EK80 signal amplitude for reducing EK60 signal amplitude, but do not extend to the same low $Power_{cal}$ levels as for Tridens (due to the shorter recording range of the G.O. Sars data). Hence, it cannot be determined from these data whether the G.O. Sars data would show the same relative increase in EK80 signal at lower signal levels. There are several sources of background noise in ship-mounted echosounder data, including echosounder self-noise, electrical noise from other systems onboard the ship, and acoustic noise such as that generated by water flow. Differences in self-noise and noise susceptibility between the EK60 and EK80, as well as differing levels of external noise on ships will likely result in ship-specific EK60 to EK80 differences at low signal levels. In the datasets presented here, the EK80 generally measures a higher level of background noise than does the EK60. It is important to note that this may not apply when the EK80 is directly connected
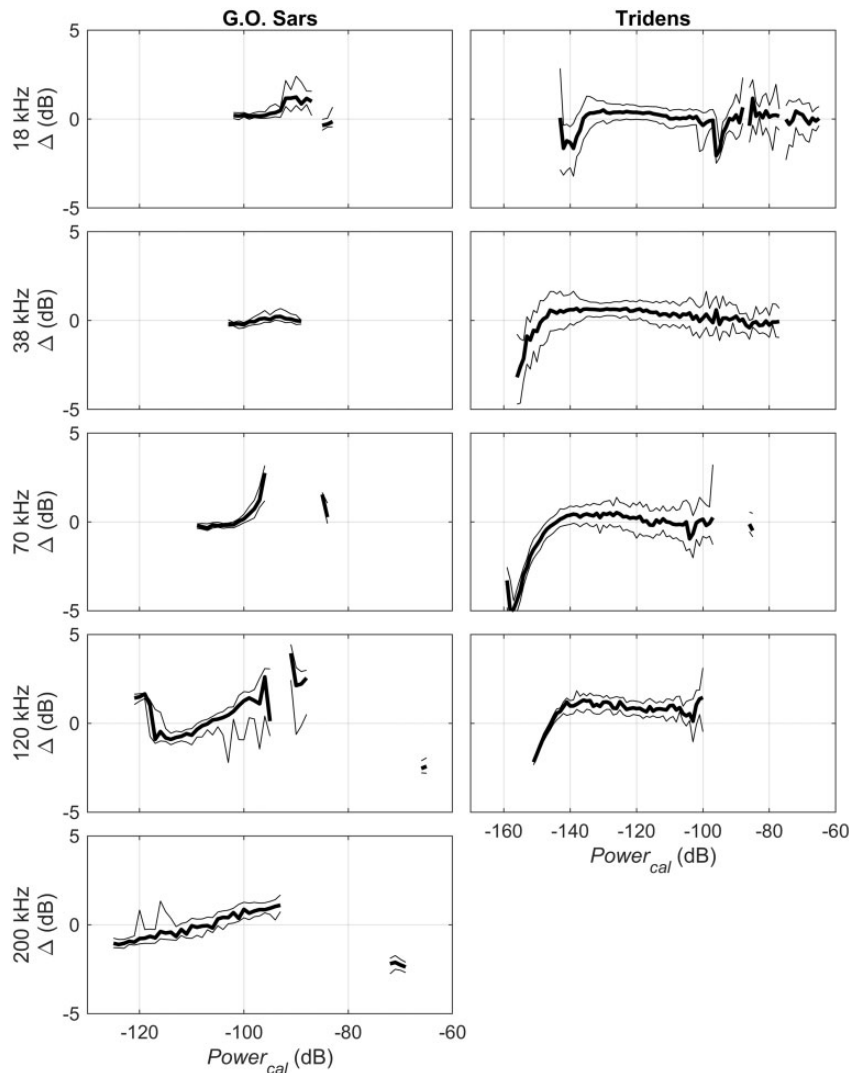
Figure 7. The median of EK60–EK80 $Power_{cal}$ (S_a with spherical spreading and absorption compensation subtracted), as a function of EK60 $Power_{cal}$ for the RV G.O. Sars and RV Tridens datasets (solid thick line) using 1 dB bins. Also shown are the 25% and 75% percentiles (thin black lines) of the differences. Bins that contain data from less than 10 cells are not shown.

to a transducer (i.e. not through a multiplexing system with associated non-optimal electrical shielding and grounding) and may vary with particulars of the echosounder installation and ship.

Calibration was carried out using the software provided by the manufacturer from multiplexed datasets and can be taken to be from near-identical sphere echoes. Several aspects of the calibration procedure have changed between the long-established EK60 process and the EK80 process and ensuring compatibility was important and required attention to detail. For example, the EK60 calibration requests an estimate of the calibration sphere target strength (dB re 1 m²) from the operator, while the EK80 requests information about the sphere and water and calculates the target strength. Community practice has been to use a target strength value calculated from a weighted average over the bandwidth of the transmit pulse (MacLennan, 1981), but the EK80 calibration software currently uses a target strength value calculated at a frequency that is slightly below the nominal echosounder operating frequency. This initially resulted in the sphere target strengths used in the EK60 and EK80 calibration software to differ by

between −0.23 and 0.29 dB re 1 m², depending on frequency, and gave erroneous offsets in the EK60 to EK80 comparisons of similar magnitudes. In addition, the sound speed that the echosounders use to estimate the sphere range can be manually specified or calculated from water property information. Providing the same water property data produced differing sound speed estimates in the EK60 and EK80 software. A similar situation occurred with the estimates of acoustic absorption, but without the option of manually entering a value. The use of consistent calibration sphere target strength, sound speed and absorption estimates in a time-series of acoustic surveys must currently be achieved by the echo-integration program, not the echosounder software. Despite the above, some comparisons show a constant offset between the EK60 and EK80 backscatter, such as the 18 and 38 kHz Tridens datasets (Figure 5). This is consistent with, but not necessarily due to, an error in the calibration process.

While the comparisons provided in this paper show good agreement between the two echosounders, initial comparisons did not and lead to further investigations to determine why. The

EK60 and EK80 provide their data in different raw forms and the conversion to calibrated backscatter is also different, requiring new conversion and calibration routines in analysis software. It is notable and informative that the most significant differences found were due to incorrect received power to s_v conversion formulae, incorrect application of these formulae in processing software, and errors in calibration calculations. This highlights that comparisons must include the entire data processing chain. The comparison of backscatter measurements between two echosounders was, at first glance, thought to be a simple task with a straightforward outcome. This was incorrect. Changing to new equipment requires a detailed and exhaustive assessment of all measurement and analysis aspects that contribute to the final output.

The close agreement of the processed data from LSSS and Echoview, when applied to the same dataset, shows that both have implemented the reading of data, application of calibration values, and integration into a grid in a consistent manner.

This work has presented a comparison of area backscatter coefficients and its use for fish biomass estimation. It has not compared performance of the echosounders for target strength estimation on resolved targets. Such a comparison would be beneficial, as has been done in conjunction with the EK60 echosounder and its predecessor, the EK500 (Jech *et al.*, 2005). For example, the EK80 supports the use of 3-sector transducers for estimating within-beam target positions, while the EK60 only supports 4-sector transducers. The effect of this on target position accuracy and variability would be of particular interest (Kieser *et al.*, 2005).

The magnitude of the differences between the EK60 and EK80 is generally less than other sources of bias and error in acoustic surveys and the stock assessment process (see Table 9.2, Simmonds and MacLennan, 2005) and hence a change from the EK60 to the EK80, with due attention to procedural differences in the calibration and configuration of the echosounders and processing of the data, should not introduce a significant change in a survey time-series biomass estimate.

The comparisons presented here have occurred on two ships over relatively short time periods. Further comparisons over longer time periods and in a wider range of backscattering conditions would provide increased confidence that the EK80 echosounder will not introduce a significant bias in fish biomass estimates derived from acoustic surveys conducted using EK60 echosounders.

Acknowledgements

Funding

References

Andersen, L. N. 2001. The new Simrad EK60 scientific echo sounder system. The Journal of the Acoustical Society of America, 109: 2336.

Demer, D. A., Berger, L., Bernasconi, M., Boswell, K. M., Chu, D., Domokos, R., Dunford, A. J. et al. 2015. Calibration of acoustic instruments. ICES Cooperative Research Report, 326, ICES 326. 130 pp.

Demer, D. A., Andersen, L. N., Bassett, C., Berger, L., Chu, D., Condiotty, J., Cutter, G. R. et al. 2017. 2016 USA-Norway EK80 workshop report: evaluation of a wideband echosounder for fisheries and marine ecosystem science. ICES Cooperative Research Report, 336. 69 pp.

De Robertis, A., and Higginbottom, I. 2007. A post-processing technique to estimate the signal-to-noise ratio and remove echosounder background noise. ICES Journal of Marine Science, 64: 1282–1291.

Hilborn, R., and Walters, C. J. 2003. Quantitative Fisheries Stock Assessment: Choice, Dynamics and Uncertainty. Springer, US, 600 pp.

Holland, P. W., and Welsch, R. E. 1977. Robust regression using iteratively reweighted least-squares. Communications in Statistics: Theory and Methods, 6: 813–827.

Jech, J. M., Foote, K. G., Chu, D., and Hufnagle, L. C. Jr. 2005. Comparing two 38-kHz scientific echosounders. ICES Journal of Marine Science, 62: 1168–1179.

Kieser, R., Mulligan, T. J., Williamson, N. J., and Nelson, M. O. 1987. Intercalibration of two echo integration systems based on acoustic backscattering measurements. Canadian Journal of Fisheries and Aquatic Sciences, 44: 562–572.

Kieser, R., Reynisson, P., and Mulligan, T. J. 2005. Definition of signal-to-noise ratio and its critical role in split-beam measurements. ICES Journal of Marine Science, 62: 123–130.

Korneliussen, R. J., Heggelund, Y., Macaulay, G. J., Patel, D., Johnsen, E., and Eliassen, I. K. 2016. Acoustic identification of marine species using a feature library. Methods in Oceanography, 17: 187–205.

MacLennan, D. N. 1981. The theory of solid spheres as sonar calibration targets. Scottish Fisheries Research Report, 22, Department of Agriculture and Fisheries for Scotland. 17 pp.

MacLennan, D. N., Fernandes, P., and Dalen, J. 2002. A consistent approach to definitions and symbols in fisheries acoustics. ICES Journal of Marine Science, 59: 365–369.

Simmonds, J., and MacLennan, D. 2005. Fisheries Acoustics. Theory and Practice, Blackwell Science, Oxford. 437 pp.

Handling editor: David Demer